Bulletin of the Geological Society of Malaysia, Volume 71, May 2021, pp. 13 - 22
DOI: https://doi.org/10.7186/bgsm71202102

Estimation of mechanical properties of sandstones from petrographic characteristics using artificial neural networks (ANNs)

Yasin Abdi*, Bijan Yusefi-Yegane, Amin Jamshidi

Department of Geology, Faculty of Sciences, Lorestan University, Khoramabad, Iran
* Corresponding author email address: abdi.ya@lu.ac.ir

Abstract: The accurate determination of strength parameters of rocks such as uniaxial compressive strength (UCS) and elastic modulus (E) using direct and laboratory methods require substantial time and cost. Therefore, the production of predictive relationships and models to forecast the UCS and E is of critical necessity in rock engineering. This study deals with the estimation of UCS and E of sandstones from petrographic characteristics by an artificial neural network (ANN) and multiple regression. For this purpose, 130 core specimens were prepared from sandstones in different locations in Iran. The specimens were tested to determine UCS, E, dry density, and porosity. Also, the petrographic studies including the determination of 11 textural and mineralogy parameters were performed on selected samples. The performance of the ANN model and regression analysis was evaluated using the criteria such as correlation coefficient (R), root mean squared error (RMSE), and variance account for (VAF). According to the ANN results, values of R, RMSE, and VAF were obtained to be 0.925, 0.089, and 97% for UCS and 0.876, 0.094, and 96% for E, respectively. In comparison, for the MLR model, the obtained R, RMSE, and VAF were 0.845, 0.101, and 95% for UCS and 0.797, 0.116, and 93% for E, respectively. A comparison between the findings illustrated that the ANN model was more suitable for forecasting the UCS and E compared with the MLR method.

Keywords: ANN, MLR, petrographic properties, UCS, modulus of elasticity, sandstone

INTRODUCTION

The uniaxial compressive strength (UCS) and elastic modulus (E) of rocks are two essential and significant geomechanical factors for rock engineering projects such as tunneling, dams, rock blasting, rock slopes, rock foundations, and underground structures. The UCS test of rock (ISRM, 1981) is the most common direct method to determine the strength of rock samples. However, determining UCS is relatively costly and destructive. Additionally, sometimes providing high-quality rock specimens is a difficult task to be accomplished, especially in the case of porous, thinly bedded, foliated, weak, and weathered rocks. These impeding factors encourage laboratory technicians to utilize easier methods (indirect techniques) for assessing the compressive strength of rocks. To overcome these difficulties, many researchers using regression techniques have estimated the UCS and E of different rocks (Brace, 1961; Hartley, 1974; Bell, 1978a; Barbour *et al*., 1979; Fahy & Guccione, 1979; Gunsallus & Kulhawy, 1984; Howarth & Rowlands, 1986; Dobereiner & DeFreitas, 1986; Cargill & Shakoor, 1990; Shakoor & Bonelli, 1991; Ulusay *et al*., 1994; Kahraman, 2001; Yasar & Erdogan, 2004; Basu & Aydin, 2006; Sharma & Singh, 2008; Kilic & Teymen, 2008; Zorlu *et al*., 2009; Yagiz, 2009; Yilmaz & Yuksek, 2009; Sarkar *et al*., 2009; Kahraman, 2014; Jahed Armaghani *et al*., 2014).

For example, Gupta & Sharma (2012) investigated the correlation between petrographical parameters with the physical and mechanical properties of quartzites selected from the northwest Himalaya. They observed that the UCS of selected rocks is strongly related (R=0.71) to the texture coefficient. Heidari *et al*. (2013) applied the regression equations to predict the UCS and E of Jurassic sandstones. They showed that textural factors such as the percentage of long contacts, packing proximity (Pp), and packing density (Pd) have the strongest correlations with most of the geoengineering parameters of selected sandstones. Also, Khanlari *et al*. (2016) indicated that the petrographic indexes of packing proximity and packing density can better predict the engineering properties of the Famenin conglomerates compared with the other characteristics.

Soft computing methods such as artificial neural networks (ANN) can be used as powerful and reliable tools to estimate the strength parameters of different rocks. ANN as a smart, low-cost, and convenient technique can be applied to predict the UCS and E of different rocks. In the recent past year, the application of artificial intelligence in the estimation of mechanical properties of different rocks has been underlined in many studies. Sometimes, to have a better evaluation, it is suggested to consider the influence of several parameters on the parameter of interest. Among different artificial intelligence techniques, many researchers suggested the feasibility of artificial neural networks (ANNs) in forecasting the UCS and E of rocks (Singh *et al*., 2001; Dehghan *et al*., 2010; Majidi & Rezaei, 2013; Torabi-Kaveh *et al*., 2014; Jahed Armaghani *et al*., 2016; Abdi *et al*., 2018). Singh *et al.* (2001) proposed an ANN-based predictive approach of UCS based on 112 sets of data. They used petrographic data to train and test their model. Dehghan *et al.* (2010) recommended the feasibility of ANN to predict UCS. They developed the model using 30 sets of data. Their input data comprise of P-wave velocity (*Vp*), point load index values, *SRn*, and porosity. They reported the coefficient of determination (R^2) value of 0.86 for this model and concluded that their predictive model is reliable enough. Using 105 sets of data, Torabi-Kaveh *et al*. (2014) constructed an ANN-based model for predicting the UCS. They used density, porosity, and V_p and the proposed model with R=0.95. In another study, Abdi *et al.* (2018) forecasted the UCS of sedimentary rocks using ANN. They tested the model on the 196 samples of limestone, conglomerate, sandstone, and marl. The inputs of their suggested model were porosity, water absorption, dry density, and P-wave velocity. The correlation coefficient, *R*, of their proposed model for testing data was 0.93. Also, Jahed Armaghani *et al*. (2016) predicted the UCS of sandstones using several modeling methods. They used the 108 datasets to develop the simple, linear, and non-linear multiple regressions, ANN, and a hybrid model constructed by integrating an empirical competitive algorithm with ANN. Finally, they concluded that the predictive accuracy of the ICA-ANN model is higher compared with the other techniques.

This work aims to develop a capable predictive ANN model for estimating the UCS and E of sandstones from different petrographic properties. To assess the prediction accuracy of the developed model, the results were compared with those of the MLR method. Petrographic parameters considered as input data are presented in Table 1.

MATERIALS AND METHODS

To perform this study, 20 sandstone blocks with dimensions of 40 cm × 40 cm × 20 cm were collected from different locations in the southwest of Qom, northeast of Hamedan (Upper Red Formation), and east of Hamedan (Jurassic sandstones) (Figure 1). Then, the collected blocks were cored in the laboratory to prepare core samples with NX size (54.1 mm diameter) and length to diameter ratio between 2.5 and 3.0 (ISRM, 1981). To develop the ANN models and MLR relationships, different physical, mechanical, and petrographical properties of 130 sandstone samples were determined according to the ISRM (1981). In this research, a multilayer perceptron (MLP) network was developed for predicting the UCS and E. An MLP is consists of at least 3 layers of nodes: an input layer, a hidden layer, and an output layer. Different ANN models have been constructed using petrographic properties as inputs for predicting the UCS and E (outputs). The petrographic parameters considered as input data include quartz content (Q), feldspar content (FL), rock fragments (RF), mean grain size (Mgs), angular degree (An), rounded degree (Ro), longitudinal contacts (Lo), concavo-convex contacts (C-C), sutured contacts (Su), packing density (P_d), and packing proximity (P_p). These parameters are not extremely destructive and rather are quick, cheap, and obtainable. In this work, the data needed for training, validation, and testing steps were selected randomly from 130 laboratory data sets. Also, 70% of the data were used for training the model, 15% for validating data set to assess the network performance, and the remaining 15% for testing the model performance.

Table 1: Petrographic parameters used in this study.

Petrographic parameter	Description
Q	Quartz content (%)
F	Feldspar content (%)
R	Rock fragments (%)
Mgs	Mean grain size (mm)
An	Angular degree (%)
Ro	Rounded degree (%)
Lo	Longitudinal contacts (%)
CC	Concavo-Convex contacts (%)
Su	Sutured contacts (%)
Pd	Packing density (%)
Pp	Packing proximity (%)

RESULTS AND DISCUSSIONS

Mineral composition

The textural properties of the rock samples were determined using an optical microscope. The results of the petrographic studies are given in Table 2. The selected sandstones were mainly composed of quartz (5.71%-

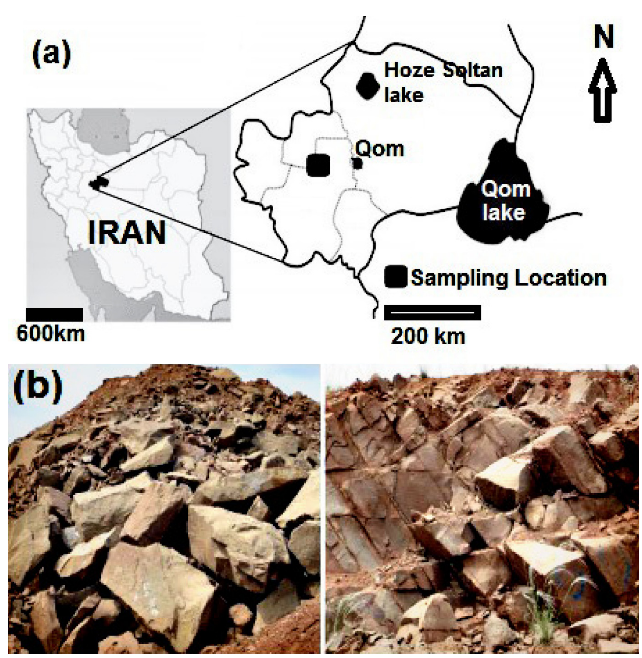

Figure 1: a) The study area and b) the pictures of sampling stations.

96.42%) and rock fragments (1.05%-84.00%). Also, the samples contain 1.16%-37.04% feldspar and 5-20% of other minerals such as clay and opaque. According to the Folk's classification (1974), the selected sandstones were classified as litharenites, feldspathic litharenites, and subarkoses. Table 2 lists the results of the textural investigations for all samples. Some petrographical aspects of the considered sandstones are shown in Figure 2.

Regarding the high number of data in this study, only some of them were chosen randomly and listed in Table 2. The results of the statistical study conducted for the original dataset are listed in Table 3. As presented in Table 2, the values of maximum, minimum, average, and standard deviation (SD) for UCS are 143.03, 19.94, 90.91, and 31.01 MPa, respectively. Also, these values for the E are 17.94, 2.93, 11.76GPa, and 3.52, respectively.

RELATIONSHIP BETWEEN PETROGRAPHIC CHARACTERISTICS AND ENGINEERING PROPERTIES

The correlation between petrographic and mechanical parameters was investigated using 11 petrographic parameters. The results of textural and modal studies are listed in Table 4. As given in this table, the UCS has a statistically significant correlation with sutured contact (r = 0.92), packing proximity (R = 0.86), and angularity of grains (R = 0.85). The petrographic indexes with the highest influence on the E also included the percentage of cement (R = 0.74), mean grain size (r = 0.70), and angularity of grains (R = 0.64).

Multiple Linear Regression (MLR)

MLR is a useful technique to construct the relationships between input and output parameters. In this study, the MLR

Table 2: The mechanical and petrographic data for some studied sandstone samples.

Sample no.	Quartz (%)	Feldspar (%)	Rock Fragments (%)	Mgs (mm)	An (%)	Ro (%)	Lo (%)	C-C (%)	Su (%)	Pd (%)	Pp (%)	UCS (MPa)	E (GPa)
S1	8.14	28.3	43.56	0.08	90	10	10	25	51	90	75	128.13	16.05
S2	10.97	17.16	58.87	0.09	87	13	13	35	42	84	68	94.61	15.71
S3	7.31	14.39	70.3	0.28	79	21	21	56	36	79	58	41.91	7.15
S4	6.23	21.91	63.86	0.18	76	24	24	25	53	86	64	72.50	9.13
S5	12.13	11.78	59.09	0.13	85	15	15	38	46	89	67	95.39	15.69
S6	7.91	24.32	49.77	0.09	88	12	12	32	43	82	73	116.68	14.83
S7	10.43	12.56	64.01	0.42	77	23	23	43	32	78	49	46.31	10.50
S8	9.65	15.24	65.11	0.35	80	20	20	45	32	77	45	19.94	2.93
S9	12.22	21.95	46.83	0.13	88	12	12	24	51	83	74	127.12	10.62
S10	11.19	23.63	48.18	0.09	90	10	10	22	54	87	70	143.03	14.24
S11	7.04	24.85	54.11	0.17	84	16	16	23	51	93	72	112.13	10.67
S12	14.43	13.72	59.85	0.38	85	15	15	40	42	81	57	69.97	9.34
S13	11.53	14.75	49.72	0.14	87	13	13	17	62	83	59	114.22	17.94
S14	10.16	16.22	57.62	0.21	84	16	16	38	40	83	63	86.13	13.67
S15	10.03	21.42	53.56	0.19	86	14	14	29	48	85	65	100.56	9.62
S16	9.16	17.02	60.98	0.20	82	18	18	38	42	83	63	77.90	12.17
S17	11.05	19.24	52.97	0.20	86	14	14	26	51	86	65	109.84	13.05
S18	9.41	17.45	59.85	0.23	82	18	18	38	41	82	61	74.26	10.12
S19	10.11	19.65	55.65	0.23	83	17	17	31	44	84	62	89.71	9.79
S20	8.16	20.44	59.15	0.08	76	10	10	17	32	77	45	84.29	12.01

Ro: Rounded degree; An: Angular degree; Lo: longitudinal contacts; C-C: Concavo-Convex contacts; Su: Sutured contacts; P_d: Packing density; P_p: Packing proximity

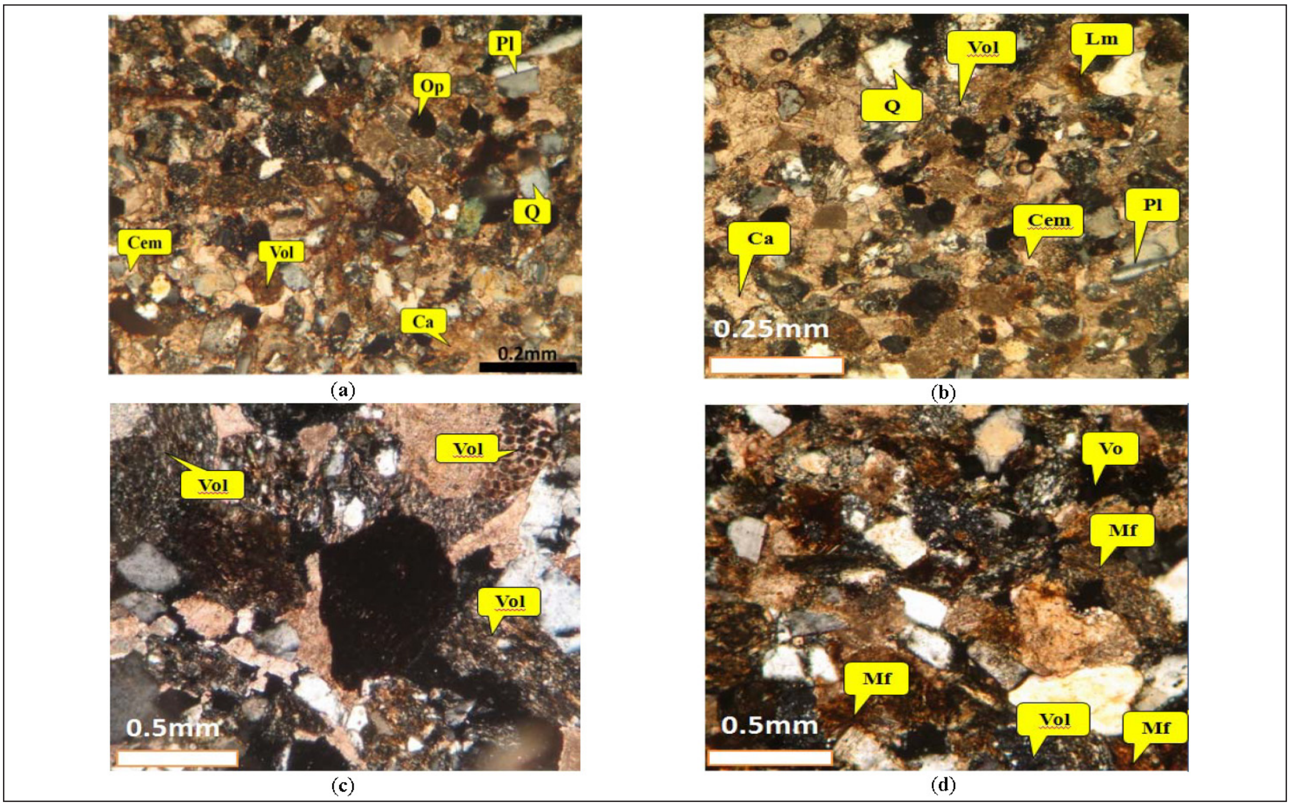

Figure 2: Petrographical images of the selected sandstones (Pl: Plagioclase, Q: Quartz, Ca: Carbonate fragment, Vol: Volcanic fragment, Mf: Metamorphic fragment, and Cem: Carbonate cement).

Table 3: The results of the statistical study conducted for the original dataset (130 samples).

Parameter	Min	Max	Ave	Std. deviation
Q (%)	5.71	96.42	34.92	27.44
F (%)	1.16	37.04	13.18	7.05
R (%)	1.05	84.00	51.90	22.86
Mgs (mm)	0.08	0.75	0.30	0.14
An (%)	58.00	92.00	78.68	8.53
Ro (%)	8.00	42.00	21.46	8.57
Lo (%)	13.00	68.60	35.21	12.50
C-C (%)	15.00	62.00	32.31	9.23
Su (%)	1.00	28.00	13.00	6.50
Pd (%)	55.15	97.80	84.36	9.71
Pp (%)	34.42	88.70	65.17	16.20
UCS (MPa)	19.94	143.03	78.78	17.69
E (GPa)	2.93	17.94	9.64	2.46

Ro: Rounded degree; An: Angular degree; Lo: longitudinal contacts; C-C: Concavo-Convex contacts; Su: Sutured contacts; P_d: Packing density; P_p: Packing proximity

Table 4: The correlation coefficient (R) between petrographical and mechanical properties.

Petrographical characteristics	R	
	UCS (MPa)	E (GPa)
Mgs (mm)	-0.815	-0.697
Q (%)	0.143	0.197
F (%)	0.652	0.180
R (%)	-0.63	-0.57
An (%)	0.847	0.643
Ro (%)	-0.847	-0.643
Pp	0.862	0.585
Pd	0.697	0.487
Su	0.916	0.618
C-C	0.788	0.566
Lo	-0.821	-0.520

Ro: Rounded degree; An: Angular degree; Lo: longitudinal contacts; C-C: Concavo-Convex contacts; Su: Sutured contacts; P_d: Packing density; P_p: Packing proximity

method was implemented for predicting UCS and E. In general, the MLR method is expressed using the relationship between output variable (Y) and input variables (Xi), which is expressed by Eq. (1):

$$Y= c + b1X1 + b2X2 + b3X3 +\ldots+ bnXn \qquad (1)$$

where *Y* is the dependent parameter, *c* is a constant value, *X1* to *Xn* are variables, and *b1* to *bn* are partial regression coefficients for *X1* to *Xn*, respectively. The optimum relations suggested predicting the UCS and E based on the MLR technique are given in Table 4. To assess the performance of developed relations, correlation coefficient (R), the root mean square error (RMSE), and variance account for (VAF) indices between predicted and measured values were determined as follows (Eqs. 2, 3 and 4):

$$R = \frac{\sum_{i=1}^{n}(X_i-\bar{X})(Y_i-\bar{Y})}{\sqrt{\sum_{i=1}^{n}(X_i-\bar{X})^2(Y_i-\bar{Y})}^2} \qquad (2)$$

$$RMSE = \sqrt{\frac{\sum_{i=1}^{n}(X_i-Y_i)^2}{n}} \qquad (3)$$

$$VAF = \left[1-\frac{var(Xi-Yi)}{var(Xi)}\right] \times 100 \qquad (4)$$

where Xi and Yi are the actual and predicted data, respectively; $\bar{X}$ and $\bar{Y}$ are mean of the measured and predicted data, respectively; and n is the number of data points. If the values of VAF and RMSE are equal to 100 and 0, respectively, the prediction performance of the model is the best. The calculated values of these indices are given in Table 5 for UCS and E. The correlation between the estimated values of the UCS and E using the MLR method (models 10 and 20 in Table 5) and the observed values in the laboratory is presented in Figure 11a and 11b, respectively. Following the results, the correlation coefficients (R) between the predicted and observed UCS and E are determined to be 0.845 and 0.797, respectively. Hence, it can be concluded that the MLR is capable of forecasting the UCS and E with acceptable precision. Also, in Figures 3c and 3d illustrate the distribution of the difference between measured and estimated UCS and E, respectively.

ANN approach

An artificial neural network (ANN) can be viewed as a black box that is utilized when there is an extremely nonlinear relationship between model inputs and model output. The term black box sometimes is given to ANNs because unlike regression-based techniques, there is no specific formula for estimating the parameter of interest. Multilayer perceptron (MLP) is the most common type of ANNS for both estimation and classification problems (Tiryaki, 2008; Mohamed, 2009; Cevik *et al*., 2011; Hajihassani *et al*., 2014). There is no specific approach for defining the number of hidden layers and also the number of nodes in the hidden layer.

In this work, the numbers of neurons in the input layer were selected to be 11, corresponding to the mentioned independent factors. In the output layer, a single node was defined based on the dependent factor (UCS or E for each network). The number of hidden layers and their neurons is determined depending on the difficulty of the studied problem. Normally, to develop an optimum network with small size and high learning capability, the hidden layers with the minimum number of neurons must be selected (Taheri *et al*., 2015). For this purpose, several combinations were constructed with different numbers of the neuron of

Table 5: The best MLR equations to predict the UCS and E.

Model no.	Equations	R	RMSE	VAF
1	UCS = 0.769CC – 46.53Mgs + 67.83	0.635	0.157	91
2	UCS = 0.78CC – 47.48Mgs – 0.04F + 68.25	0.635	0.156	91
3	UCS = 0.76CC – 40.48Mgs – 0.18F – 0.29Lo + 78.86	0.658	0.154	92
4	UCS = 0.72CC – 44.96Mgs + 0.13F – 0.46Lo + 0.17Q + 77.62	0.673	0.142	93
5	UCS = 0.71CC – 44.95Mgs - 0.04F – 0.46Lo – 0.17L+ 0.12Q + 94.78	0.681	0.140	93
6	UCS = 0.33CC – 41.63Mgs - 0.42F – 1.12Lo – 0.22L – 1.12Ro + 0.06Q + 161.212	0.761	0.133	94
7	UCS = 0.41CC – 42.09Mgs - 0.47F – 1.19Lo – 0.28L – 5.88Ro + 0.22Q – 4.81An + 645.91	0.795	0.112	95
8	UCS = 0.37CC – 55.41Mgs - 0.55F – 1.43Lo – 0.13L – 5.97Ro + 0.31Q – 5.51An + 0.66Pp + 667.29	0.826	0.107	95
9	UCS = 0.41CC – 56.74Mgs - 0.72F – 1.45Lo – 0.09L – 6.09Ro + 0.47Q – 5.48An + 1.24Pp – 1.04Pd + 717.54	0.840	0.104	95
10	UCS = 0.25CC – 56.12Mgs - 0.68F – 1.69Lo – 0.109L – 6.04Ro + 0.30Q – 5.32An + 1.45Pp – 0.93Pd – 0.60Su + 701.18	0.845	0.101	95
11	E = -6.37Mgs – 0.08Lo +14.47	0.681	0.231	85
12	E = -5.06Mgs – 0.07Lo + 0.09CC +10.71	0.749	0.138	88
13	E = -6.28Mgs – 0.09Lo + 0.094CC + 0.02Q +11.05	0.760	0.129	89
14	E = -7.80Mgs – 0.083Lo + 0.13CC + 0.13Q + 0.13L – 0.419	0.790	0.129	90
15	E = -7.95Mgs – 0.09Lo + 0.123CC + 0.133Q + 0.134L + 0.008Pp – 0.946	0.790	0.129	90
16	E = -7.952Mgs – 0.09Lo + 0.123CC + 0.130Q + 0.001L + 0.008Pp – 1.34F – 12.40	0.790	0.129	90
17	E = -7.923Mgs – 0.083Lo + 0.127CC + 0.132Q + 0.001L - 0.002Pp – 1.35F + 0.019Su– 12.49	0.791	0.118	93
18	E = -7.854Mgs – 0.086Lo + 0.125CC + 0.133Q + 0.000L - 0.004Pp – 1.36F + 0.016Su – 0.007Ro– 12.942	0.791	0.117	93
19	E = -7.838Mgs – 0.085Lo + 0.124CC + 0.131Q + 0.000L - 0.004Pp – 1.35F + 0.015Su – 0.022Ro + 0.03An – 10.004	0.791	0.117	93
20	E = -7.976Mgs – 0.081Lo + 0.133CC + 0.129Q + 0.004L - 0.042Pp – 0.152F + 0.031Su – 0.009Ro + 0.028An – 0.042Pp – 15.001	0.797	0.116	93

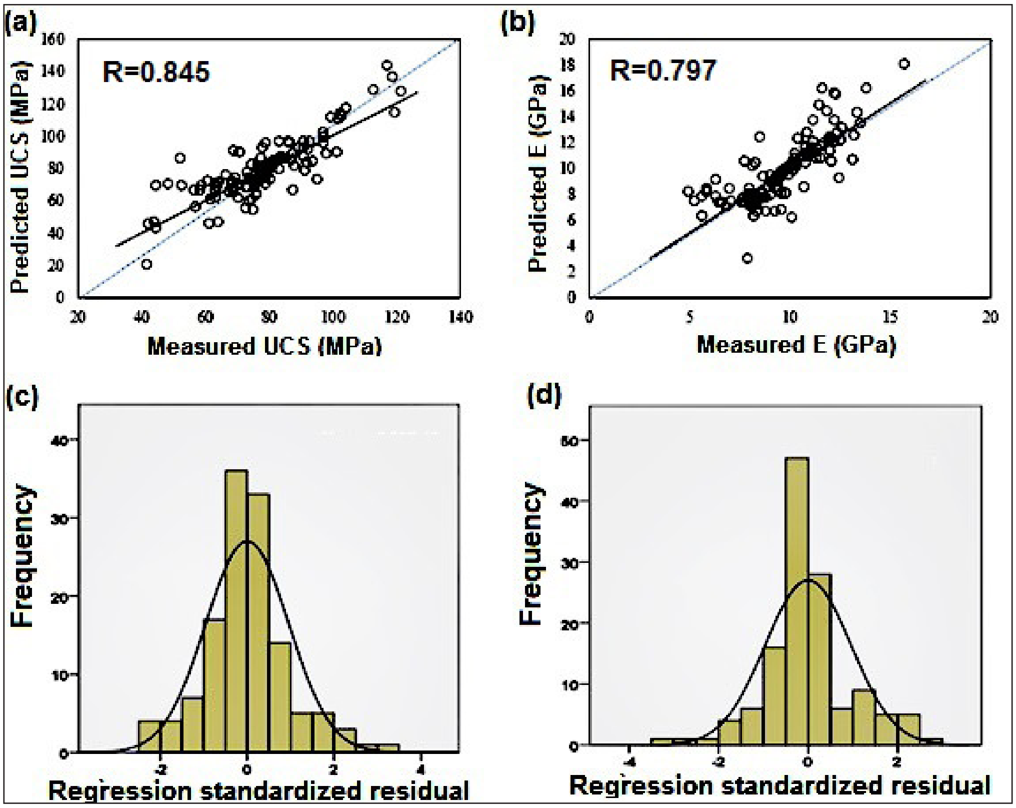

Figure 3: The R between measured and predicted values of a) UCS and b) E using the MLR method (models 10 and 20, Table 5); c) and d) the difference between measured and predicted UCS and E from the MLR method, respectively.

one hidden layer to obtain the ideal ANN structure. Based on this, the work was started with at least two neurons and, finally, the neurons increased up to 10 using the trial and error technique. To achieve the best architecture, the RMSE and R were considered as the selection criteria. In this regard, the selection process of the number of neurons in the hidden layer(s) is most significant and tedious. Selecting a too restricted or excessive number of neurons within the hidden layers can cause under- or over-fitting of the model, respectively. Besides, a sizable amount of neurons within the hidden layer can take more machine training time. For the optimization of the network in the training step, it is necessary to optimize the number of neurons in the hidden layer. Finally, 10 neurons were designated as the ideal number in the hidden layer with the maximum R-value and the lowest value of RMSE. Figure 4 depicts the ideal network structure to forecast the UCS and E of studied sandstones. As shown in this figure, the structure 11-10-1 is the smallest network with maximum prediction accuracy. To assess the estimation accuracy and performance of the constructed network, the indices RMSE and R were used. In general, an ideal network is recognized with the minimum value of RMSE and maximum value of R. Based on this, R-value larger than 0.9 indicates the best performance of the network, R-value between 0.8 and 0.9 describes a good performance,

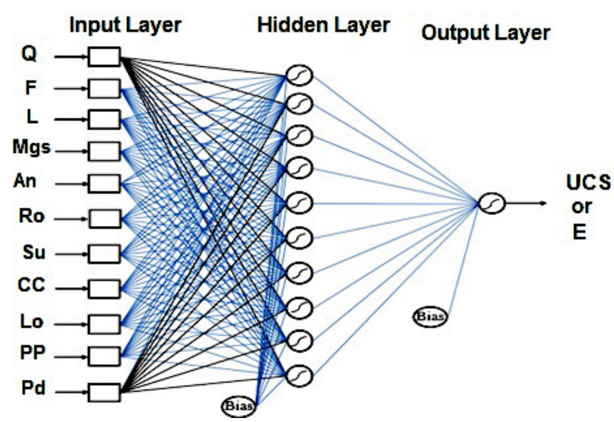

Figure 4: The structure of ANN developed in this study.

and R-value less than 0.8 indicates an unacceptable efficiency of the network (Ahmadi *et al*., 2013). The entire information on optimum network architecture is summarized in Table 6.

In this study, 30% of the data were randomly selected for testing and validating the constructed ANN model. It is important to note that these data were not used for training the network. The results of network performance for predicting the UCS and E of selected sandstones are given in Figures 5 and 6, respectively. As can be seen in these figures, R between the predicted and actual values of UCS and E is used for assessing the network performance. Based on the results, the R values in training, validation, and testing steps for *UCS* are 0.994, 0.898, and 0.925, respectively. These values for *E* are 0.979, 0.930, and 0.876, respectively (Figure 6).

Table 6: Information about optimum network architecture.

Number of input neurons	11
Number of hidden layers	1
Number of hidden neurons	10
Number of output neurons	1
Number of training epochs	400
Number of training datasets	90
Number of testing datasets	20
Number of validation datasets	20
Training function	Levenberg–Marquardt back-propagation
Transfer function	LOGSIG
Learning rate	0.1
Error goal	10^{-6}

The comparison of ANN and MLR methods

To assess the performance of the models developed in this work, three statistical performance evaluation indices, namely R, RMSE, and VAF were utilized. The results of this comparison are listed in Table 7. According to the results, the MLR and ANN can forecast UCS and E values with high accuracy. A comparison of the results shows that the ANN performance is better than the MLR and runs results closer to the actual values.

CONCLUSIONS

In this study, a model was developed to predict UCS and E of sandstones using an artificial neural network (ANN) technique. For this purpose, 11 petrographic parameters of 130 core samples were used for modeling the UCS and E. Also, the ANN results by the neural network were compared with the results obtained by regression analysis (MLR). Based on the multiple regression analysis (MLR), two empirical relationships were developed to estimate the UCS and E of the selected sandstones:

UCS = 0.25CC – 56.12Mgs - 0.68F – 1.69Lo – 0.109L – 6.04Ro + 0.30Q – 5.32An + 1.45Pp – 0.93Pd – 0.60Su + 701.18

E = -7.976Mgs – 0.081Lo + 0.133CC + 0.129Q + 0.004L - 0.042Pp – 0.152F + 0.031Su – 0.009Ro + 0.028An – 0.042Pp – 15.001

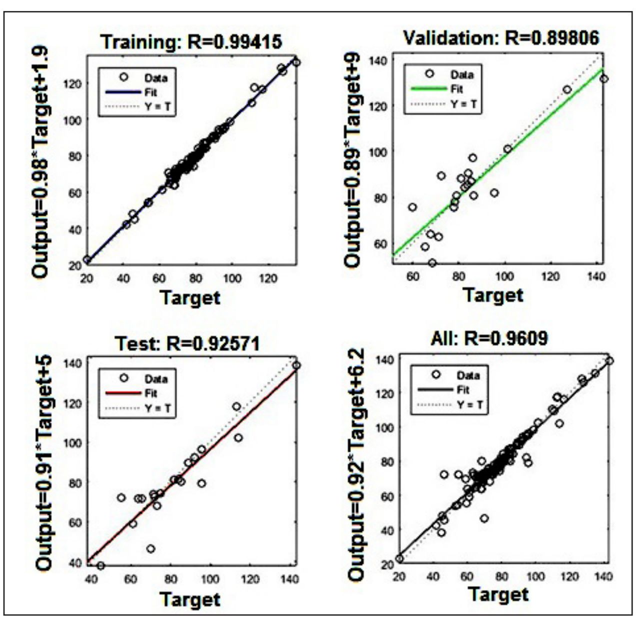

Figure 5: The prediction results of the ANN for UCS.

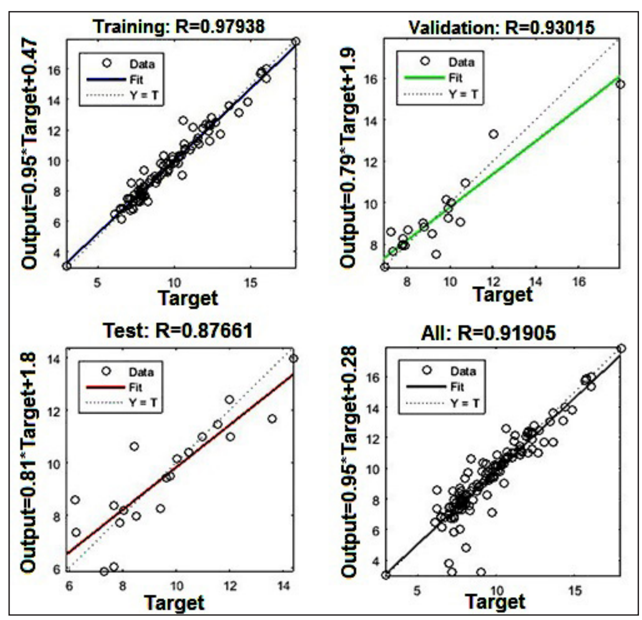

Figure 6: The prediction results of the ANN for E.

Table 7: The results of the R, RMSE, and MAE for the ANN and MLR techniques.

Analysis	UCS (MPa)			E (GPa)		
	R	RMSE	VAF	R	RMSE	VAF
MLR	0.845	0.101	95	0.797	0.116	93
ANN (train)	0.994	0.015	98	0.979	0.041	97
ANN (test)	0.925	0.089	97	0.876	0.094	96

To evaluate the predictive performance of the two methods used in this study, three statistical indices of R, RMSE, and VAF were used. According to the results of ANN, the R values for the UCS and E were 0.925 and 0.876, respectively. These values indicate higher prediction reliability than the MLR method as it provided the R values of 0.845 and 0.749 for UCS and E, respectively. Furthermore, comparing the results of other statistical indices confirms that network performance is much better than the MLR. According to these results, it is concluded that ANN can be applied as a smart, low cost, and convenient technique to estimate the UCS and E of sandstones.

ACKNOWLEDGEMENTS

The authors would like to acknowledge the financial support of Lorestan University for this research under grant number 98403421. We also thank the anonymous reviewers for their constructive comments and suggestions.

REFERENCES

Abdi, Y., Garavand, A.T. & Sahamieh. R.Z., 2018. Prediction of strength parameters of sedimentary rocks using artificial neural networks and regression analysis. Arab J. Geosci., 11, 587.

Ahmadi, M.A., Ebadi, M., Shokrollahi, A. & Majidi, S.M.J., 2013. Evolving artificial neural network and imperialist competitive algorithm for prediction oil flow rate of the reservoir. Applied Soft Computing, 13, 1085–1098.

Barbour, T.G., Atkinson, R.H. & Ko, H.Y., 1979. Relationship of mechanical, index and mineralogic properties of coal measure rock. 20th Symp. Rock Mechanics, Austin, Tex., 189-198.

Basu, A. & Aydin, A., 2006. Predicting uniaxial compressive strength by point load test: significance of conepenetration. Rock Mech. Rock Eng., 39, 483–490.

Bell, F.G., 1978a. The physical and mechanical properties of the Fell Sandstones, Northumberland, England. Eng. Geol., 12, 1–29.

Brace, W.F., 1961. Dependence of fracture strength of rocks on grain size. Proc. 4th Syrup. Rock Mechanics, Univ. Park, Penn., 99-103.

Cargill, J.S. & Shakoor, A., 1990. Evaluation of empirical methods for measuring uniaxial compressive strength of rock. Int. J. Rock Mech. Min. Sci. Geomech. Abstr., 27, 495-503.

Cevik, A., Sezer, E.A., Cabalar, A.F. & Gokceoglu, C., 2011. Modeling of the uniaxial compressive strength of some clay-bearing rocks using neural network. Appl. Soft Comput., 11, 2587–2594.

Dehghan, S., Sattari, G.H., Chehreh, C.S. & Aliabadi, M.A., 2010. Prediction of unconfined compressive strength and modulus of elasticity for Travertine samples using regression and artificial neural networks. Min. Sci. Technol., 20, 41–46.

Dobereiner, L. & DeFreitas, M.H., 1986. Geotechnical properties of weak sandstones. Geotechnique, 36, 79-94.

Fahy, M.P. & Guccione, M.J., 1979. Estimating strength of sandstone using petrographic thin-section data. Bull. Assoc. Eng. Geol., 16, 467-485.

Folk, R.L., 1974. Petrology of sedimentary rocks. Hemphill Publishing Company, Austin. 182 p.

Gunsallus, K.L. & Kulhawy, F.H., 1984. A comparative evaluation of rock strength measures. Int. J. Rock Mech. Min. Sci. Geomech. Abstr., 21, 233-248.

Gupta, V. & Sharma, R., 2012. Relationship between textural, petrophysical and mechanical properties of quartzites: A case study from northwestern Himalaya. Eng. Geol., 135-136, 1–9.

Hajihassani, M., Jahed Armaghani, D., Sohaei, H., Tonnizam Mohamad, E. & Marto, A., 2014. Prediction of airblast-overpressure induced by blasting using a hybrid artificial neural network and particle swarm optimization. Appl. Acoust., 80, 57–67.

Hartley, A., 1974. A review of geological factors influencing the mechanical properties of road surface aggregation. Q. J. Eng. Geol., 7, 69-100.

Heidari, M., Momeni, A.A., Rafiei, B., Khodabaksh, H. & Torabi-Kaveh, M., 2013. Relationship Between Petrographic Characteristics and the Engineering Properties of Jurassic Sandstones, Hamedan, Iran. Rock Mech. Rock Eng., 46, 1091–1101.

Howarth, D.F. & Rowlands, J.C., 1986. Development of an index to quantify rock texture for assessment of intact rock properties. Geotech. Testing J., 9, 169–179.

International Society for Rock Mechanics (ISRM), 1981. Rock characterization, testing and monitoring, ISRM suggested methods. In: Brown, E.T. (Ed.), Pergamon Press, Oxford. 211p.

Jahed Armaghani, D., Tonnizam Mohamad, E., Momeni, E., Narayanasamy, M.S. & Mohd Amin, M.F., 2014. An adaptive neuro-fuzzy inference system for predicting un-confined compressive strength and Young's modulus: a study on Main Range granite. Bull. Eng. Geol. Environ., 74(4), 1301–1319. http://dx.doi.org/10.1007/ s10064-014-0687-4.

Jahed Armaghani, D., Mohd Amin, M.F., Yagiz, S., Shirani Faradonbeh, R. & Abdullah, R.A., 2016. Prediction of the uniaxial compressive strength of sandstone using various modeling techniques. International Journal of Rock Mechanics & Mining Sciences, 85, 174–186.

Kahraman, S., 2001. Evaluation of simple methods for assessing the uniaxial com pressive strength of rock. Int. J. Rock Mech. Min. Sci., 38, 981–994.

Kahraman, S., 2014. The determination of uniaxial compressive strength from point load strength for pyroclastic rocks. Eng. Geol., 170, 33–42.

Khanlari, G.R., Heidari, M., Noori, M. & Momeni, A., 2016. The Effect of Petrographic Characteristics on Engineering Properties of Conglomerates from Famenin Region, Northeast of Hamedan, Iran. Rock Mech. Rock Eng., 49, 2609.

Kilic, A. & Teymen, A., 2008. Determination of mechanical properties of rock susing simple methods. Bull. Eng. Geol. Environ., 67(2), 237–244.

Majidi, A. & Rezaei, M., 2013. Prediction of unconfined compressive strength of rock surrounding a roadway using artificial neural network. Neural Comput. & Applic., 23, 381–389.

Mohamed, M.T., 2009. Artificial neural network for prediction and control of blasting vibrations in Assiut (Egypt) limestone quarry. Int. J. Rock Mech. Min. Sci., 46, 426-431.

Rezaei, M., Majdi, A. & Monjezi, M., 2012. An intelligent approach to predict unconfined Compressive Strength of Rock Surrounding Access Tunnels in Longwall Coal Mining. Neural Comput. Appl., 24, 233–241.

Sarkar, K., Singh, T.N. & Reddy, D.V., 2009. Prediction of strength parameters by dynamic wave. Int. J. Earth Sci. Eng., 2(1), 12–19.

Shakoor, A. & Bonelli, R.E., 1991. Relationship between petrophysical characteristics, engineering index properties and mechanical properties of selected sandstones. Bull. Assoc. Eng. Geol., 28, 55–71.

Sharma, P.K. & Singh, T.N., 2008. A correlation between P-wave velocity, impact strength index, slake durability index and uniaxial compressive strength. Bull. Eng. Geol. Environ., 67, 17–22.

Singh, V.K., Singh, D. & Singh. T.N., 2001. Prediction of Strength Properties of Some Schistose Rocks from Petrographic Properties Using Artificial Neural Networks. Int. J. Rock Mech. Min. Sci., 38, 269–284.

Taheri-Garavand, A., Ahmadi, H., Omid, M., Mohtasebi, S.S., Mollazade, K., Russell Smith, J.R. & Carlomagno, G.M., 2015. An intelligent approach for cooling radiator fault diagnosis based on infrared thermal image processing technique. Appl. Therm. Eng., 87, 434–443.

Tiryaki, B., 2008. Predicting intact rock strength for mechanical excavation using multivariate statistics, artificial neural networks and regression trees. Eng. Geol., 99, 51–60.

Torabi-Kaveh, M., Naseri, F., Saneie, S. & Sarshari. B., 2014. Application of Artificial Neural Networks and Multivariate Statistics to Predict UCS and E Using Physical Properties of Asmari limestones. Arab J. Geosci., 8, 2889.

Ulusay, R., Tureli, K. & Ider, M.H., 1994. Prediction of engineering properties of a selected litharenite sandstone from its petrographic characteristics using correlation and multivariable statistical techniques. Eng. Geol., 37, 135–157.

Yagiz, S., 2009. P-wave velocity test for the assessment of some geotechnical properties of rock materials. Bull. Mat. Sci., 34, 947–953.

Yasar, E. & Erdogan, Y., 2004. Estimation of rock physio-mechanical properties using hardness methods. Eng. Geol., 71, 281–288.

Yilmaz, I. & Yuksek, G., 2009. Prediction of the strength and elasticity modulus of gypsum using multiple regression, ANN, and ANFIS models. Int. J. Rock Mech. Min. Sci., 46(4), 803–810.

Zorlu, K., Gokceoglu, C., Ocakoglu, F., Nefeslioglu, H.A. & Acikalin, S., 2008. Prediction of uniaxial compressive strength of sandstones using petrography-based models. Eng. Geol., 96, 141-158.

Manuscript received 22 February 2020
Revised manuscript received 16 July 2020
Manuscript accepted 12 September 2020